






ORIGINAL RESEARCH

Comparison of healing of acute total tympanic membrane perforation between rats with and without excision of the malleal handle

Zihan Lou MD^{1,2,3,4}  | Chunyan Li MD, PhD^{1,2,3,4}  | Dongzhen Yu MD, PhD^{1,2,3,4} |
Jingjing Wang MD^{1,2,3,4}  | Zhengnong Chen MD, PhD^{1,2,3,4}  |
Shankai Yin MD, PhD^{1,2,3,4} 

¹Department of Otolaryngology-Head and Neck Surgery, Shanghai Sixth People's Hospital Affiliated to Shanghai Jiao Tong University School of Medicine, Shanghai, China

²Department of Otolaryngology-Head and Neck Surgery & Center of Sleep Medicine, Shanghai Sixth People's Hospital Affiliated to Shanghai Jiao Tong University School of Medicine, Shanghai, China

³Otolaryngological Institute of Shanghai Jiao Tong University, Shanghai, China

⁴Shanghai Key Lab Sleep Disordered Breathing, Shanghai, China

Correspondence

Zhengen Chen, Department of Otolaryngology-Head and Neck Surgery, Shanghai Jiao Tong University Affiliated Sixth People's Hospital, Otolaryngology Institute of Shanghai Jiao Tong University, 600, Yishan Road, Shanghai 200233, China.
Email: jasley@126.com

Funding information

Shanghai Medical Innovation Project, Grant/Award Number: 22Y11902100; National Natural Science Foundation of China, Grant/Award Number: 82071040

Abstract

Objective: We compared the histological changes and hearing restoration during the healing of acute total tympanic membrane (TM) perforations between Sprague-Dawley (SD) rats with and without excision of the malleal handle.

Materials and methods: Bilateral, acute, and total TM perforations were created in 36 male SD rats. The malleal handle was preserved in the left ear (handle-preserved ear [HPE]) and excised from the right ear (handle-excised ear [HEE]). Endoscopic examination, auditory brainstem response (ABR) thresholds, histopathological, and scanning electron microscope (SEM) analysis were performed.

Results: Endoscopic photographs showed that all perforations in the 18 SD rats were closed. The mean closure times were 6.83 ± 0.85 and 8.50 ± 0.71 days in the HPE and HEE groups, respectively ($p < .001$). SEM images showed radial arrangement of fiber bundles in a single direction in HPEs, although normal arrangement was not achieved. In contrast, HEEs showed disorganized arrangement. At 1 month after perforation closure, the ABR thresholds at high frequencies were significantly higher in the HEE group than in the HPE group ($p = .029$ and $p = .017$ for 16 and 32 kHz, respectively). Additionally, the changes in ABR threshold were significantly different at high frequencies ($p = .011$ and $p = .017$ for 16 and 32 kHz, respectively) before and 1 month after perforation closure between the HPE and HEE groups, although the differences were not statistically significant at the remaining frequencies.

Conclusion: Although the malleus handle may not affect the closure of total perforation in SD rats, it contributes to accelerate the perforation closure by possible guide the migration of proliferative epithelial cell on the upper halves of the annulus. Additionally, resection of the malleus handle impairs high frequency hearing recovery following spontaneous closure of the TM.

Zihan Lou and Chunyan Li contributed equally to this work.

This is an open access article under the terms of the [Creative Commons Attribution-NonCommercial-NoDerivs](https://creativecommons.org/licenses/by-nc-nd/4.0/) License, which permits use and distribution in any medium, provided the original work is properly cited, the use is non-commercial and no modifications or adaptations are made.

© 2023 The Authors. *Laryngoscope Investigative Otolaryngology* published by Wiley Periodicals LLC on behalf of The Triological Society.

KEYWORDS

keratinocyte, malleus handle, spontaneous healing, tympanic membrane

1 | INTRODUCTION

The tympanic membrane (TM) is a unique structure that is suspended in air¹ and plays a role in sound collection and conduction. TM perforations typically impair hearing.^{2,3} In contrast to acute TM perforations in humans, perforations in Sprague–Dawley (SD) rats usually heal spontaneously, although the results of some studies suggest that large perforations fail to close.^{2,4}

Perforation closure may be affected by several factors, including perforation size, site, and infection.^{2–5} Recent findings suggest that the malleus handle is closely associated with TM healing and plays an important role in perforation closure in SD rats.^{2–6} Therefore, partial excision of the malleus handle may result in a nonhealing perforation.^{7,8} It is unclear whether the malleus handle affects hearing outcomes after tympanoplasty; the results of some studies suggest that the absence of a malleus handle does not affect postoperative hearing restoration,^{9,10} whereas the results of other studies suggest that hearing outcomes are improved when the malleus handle is preserved.^{11,12} However, previous studies have focused on small-to-medium-sized perforations with malleus handle preservation.^{2–8} Small perforations usually heal rapidly^{2–8} and may not accurately reflect the effects of the malleus handle. To our knowledge, no previous studies have evaluated spontaneous healing outcomes after acute total TM perforation and complete excision of the malleus handle in SD rats. This study compared histological changes and hearing outcomes after acute total TM perforation between SD rats with excised and preserved malleus handles.

2 | MATERIALS AND METHODS

2.1 | Animal model preparation

The study protocol was approved by the Animal Ethics Committee of the Otolaryngological Institute of Shanghai Jiao Tong University. In total, 36 male SD rats (*Rattus norvegicus*) weighing 250–300 g were obtained from the Animal Resources Center of the Otolaryngological Institute of Shanghai Jiao Tong University. The animals were housed in a dedicated and secure animal resources facility at the Otolaryngological Institute of Shanghai Jiao Tong University. The rats were provided food and water ad libitum under a 12-h light/dark cycle. Before perforation, all ears were examined using an otomicroscope (Carl Zeiss Meditec, Jena, Germany) for signs of otitis media, including TM inflammation and middle ear effusion. No rats were excluded from analysis, and none of the ears had infection or inflammation. The procedures were performed with the rats under general anesthesia achieved by administration of intraperitoneal pentobarbital (60 mg/kg). Similar total TM perforations of pars tensa were created in both ears using a sterile 23-gauge needle under a microscope. The malleus handle and lateral process was removed from the right ear (handle-excised ear [HEE]) and preserved in the left ear (handle-preserved ear [HPE]). The malleus handle was cut off using micro scissors and then removed gently using microsurgery forceps, the incudostapedial joint and stapes could not be damaged during excision. All the perforations were not grafted and were left to spontaneously heal.

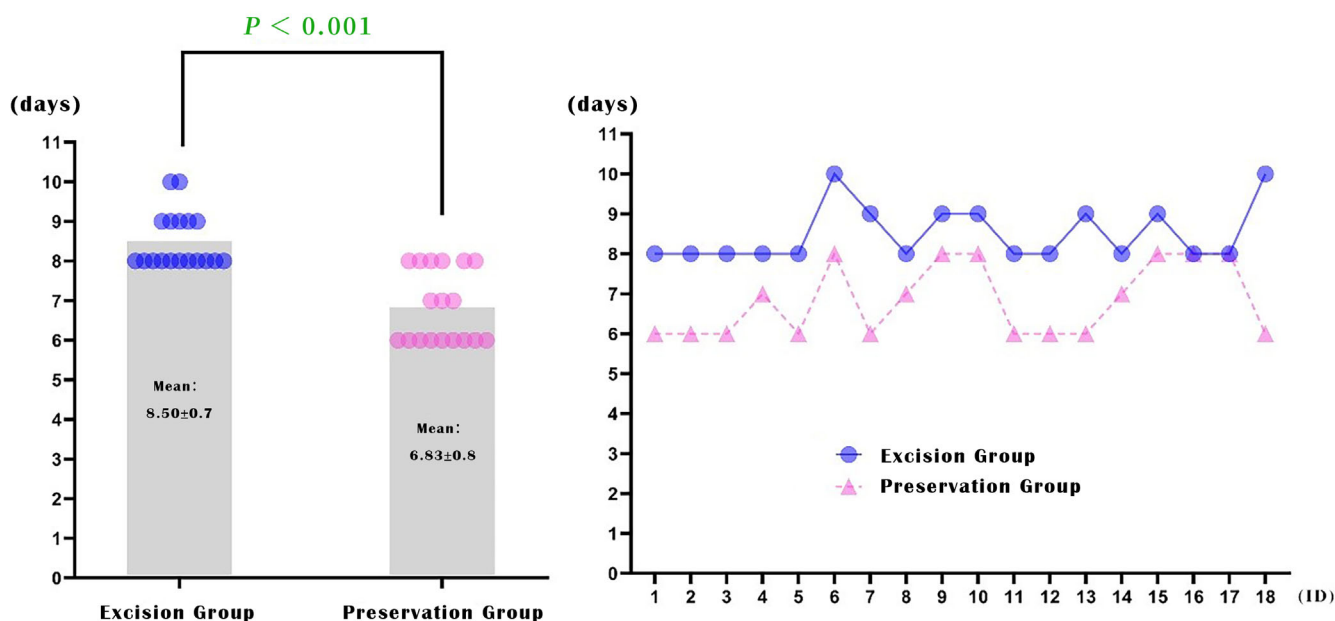


FIGURE 1 The closure times of the perforations in all ears.

2.2 | Morphological analysis

The perforation day was regarded as day 0. Closure was defined as complete endoscopic closure without intervention. Each TM was endoscopically photographed in the late afternoon before and immediately after the procedure, then daily until the perforations closed. The shape of the original perforation was evaluated immediately after the procedure.

2.3 | Histological analysis

For histopathological evaluation, three rats were sacrificed at each time point on days 3, 5, 7, 9, and 11 after perforation. Bilateral TMs and the attached annuli were extracted without damaging them. The tissues were immediately fixed in 4% (v/v) paraformaldehyde (Sangon Biotech, Shanghai, China; pH = 7.2) at 4°C for 24 h, decalcified in 10% (w/v) ethylenediaminetetraacetic acid (Sangon Biotech; pH = 7.2) at 4°C for 2 weeks, and subjected to routine paraffin histological analysis. Tissue sections (5 μ m) were stained with hematoxylin and eosin, then digitally scanned using an Aperio ScanScope XT (Leica Microsystems, Wetzlar, Germany; 20 \times /0.75 Plan Apo objective).

2.4 | Scanning electron microscope (SEM) analysis

For SEM analysis, three rats each were sacrificed at 1 month after perforation closure. Bilateral healed TMs were fixed using paraformaldehyde, dehydrated in ethanol, dried using hexamethyldisilazane solution, sputter coated with gold palladium, and examined under an SEM (Regulus 8100; Hitachi, Ltd., Tokyo, Japan).

2.5 | Auditory brainstem responses (ABRs)

The ABR thresholds of the six rats were determined at the same time points as the morphological analysis: immediately before perforation, after perforation, and 1 month after perforation closure. TMs exhibiting abnormal ABR thresholds before perforation were excluded. An RZ6/BioSigRZ system (Tucker–Davis Technologies, Gainesville, FL) was used to control stimuli and monitor responses. A speaker (MF1; Tucker–Davis Technologies) was used to generate tone-burst stimuli with parameters described previously (duration: 10 ms; rise/fall time: 0.5 ms; frequency: 21.1/s). The sounds were delivered using a coupler tip sealed to the ear canal. The resulting biological signals were recorded using a subdermal recording electrode system that was fixed at the vertex. The reference and grounding electrodes were placed posterior to the external auditory canal. Evoked responses were amplified 20-fold using a PA4 preamplifier (Tucker–Davis Technologies) and repeated 800 times. The stimulus intensity decreased from 90 to 0 dB SPL in decrements of 5 dB. The lowest stimulus that evoked an ABR wave III, repeated three times, was regarded as the ABR threshold. The tests were performed at 1, 2, 4, 8, 16, and 32 kHz.

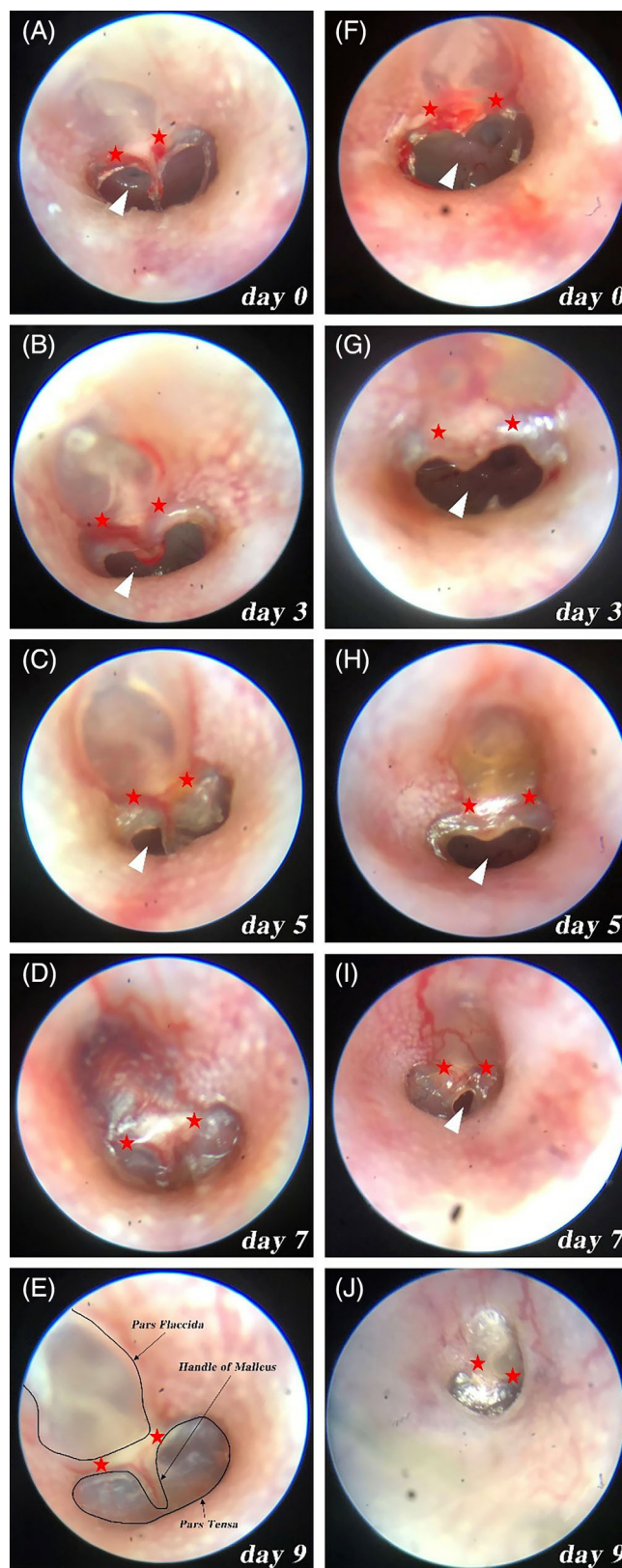


FIGURE 2 Endoscopic imaging of rat TMs via the external auditory canal (EAC). The images were captured at various timepoints. (A–E): Images of the HPE group. (F–J) Images of the HEE group. The white triangles indicate the perforations. The red pentagrams indicate the anterior and posterior malleolar folds.

2.6 | Statistical analysis

Quantitative variables are expressed as means \pm standard deviations. Paired samples *t*-tests were used to compare healing time, ABR thresholds, and threshold shift before perforation, after perforation, and after perforation closure at each test frequency between HEEs and HPEs. The threshold for statistical significance was set at $p < .05$. Statistical analysis was performed using SPSS software (version 23; IBM Corp., Armonk, NY, USA). Figures were prepared using GraphPad software (version 8.0.1; GraphPad Software Inc., San Diego, CA).

3 | RESULTS

3.1 | Healing outcomes

All 18 SD rats underwent daily endoscopic examination. All perforations closed completely; compared with the lower half, the upper half of the perforations healed more rapidly in all rats. The healed TM had original conical shapes with the transparent reflection point in HPEs and flat shapes with no transparent reflection point in HEEs. The mean closure times were 6.83 ± 0.85 (range 6–8) days in HPEs and 8.50 ± 0.71 (range 8–10) days in HEEs ($p < .001$; Figure 1). Compared with the anterior half, the posterior half of the TM exhibited more rapid healing in 15 HPEs (83.3%, 15/18); there was no significant difference between halves in the remaining 3 HPEs (16.7%, 3/18). Compared with the anterior half, the posterior half exhibited more rapid healing in 13 HEEs (72.2%, 13/18); there was no significant difference in 3 HEEs (16.7%, 3/18), whereas 2 HEEs exhibited more rapid healing in the anterior half (11.1%, 2/18).

3.2 | Morphological analysis

Eighteen SD rats underwent daily endoscopic morphological assessment.

HPEs: The pars tensa of TM left the similar U-shaped original perforation immediately after the procedure because of the presence of handle of malleus. For the appearance of the egenerated ear drum, the perforation edges were swollen near the malleus and thickened near the annulus at 3 days after perforation, particularly in the upper

half of the annulus. Epithelial layer proliferation was observed near the annulus, particularly in the upper halves of the annulus and extending over the malleal handle by day 5. An epithelial bridge was observed between the umbo and the inferior annulus, which divided the perforation into two ovals. The posterior half was closed in some rats at day 5. The perforations were closed in 9, 3, and 6 ears on days 6, 7, and 8, respectively (Figure 2(A)–(E)).

HEEs: The pars tensa of TM formed similar kidney-shaped original perforation immediately after the procedure because of the absence of the malleus. Epithelial layer proliferation was observed near the annulars on day 3 after perforation, particularly in the upper half of the annulus. The epithelial layer continued to increase and thicken on days 5 and 7, particularly in the upper half of the annulus. The perforations were closed in 0, 11, 5, and 2 ears on days 7, 8, 9, and 10, respectively.

3.3 | Histological analysis

The epithelial layer was only one cell thick in normal rat TM (Figure 3). Three rats were sacrificed for the histological analysis at each time point on days 3, 5, 7, 9, and 11 after perforation.

HPEs: The epithelial layer exhibited substantial hyperplasia near the annulus at day 3, particularly in the upper half, and was approximately 3–5 keratinocyte cells thick. The perforation appeared almost normal near the malleus. A bridge composed of proliferating keratinocytes was apparent near the annulus at day 5, whereas few keratinocytes were also present near the malleus. The connective tissue layer was mainly composed of disorganized fibroblasts. On day 7, the perforation was macroscopically closed; keratinocyte proliferation was active near the annulus and less prominent around the malleus handle. The connective tissue layer contained various cells resembling fibroblasts; fibroblasts were occasionally organized and aggregated. The TM became thinner by day 9, and more nascent keratinocytes were present at the annulus than at the malleus handle. On day 11, the epithelial layer had 1–2 flattened keratinocytes and the fibroblasts were organized (Figure 4(A)–(E)).

HEEs: The epithelial layer exhibited substantial hyperplasia near the annulus at day 3, particularly in the upper half of the annulus, with approximately 6–8 rows of keratinocytes. There was an increasing number of proliferative keratinocytes without a proliferating keratinocyte bridge on day 5. A hyperplastic epithelial layer was observed near

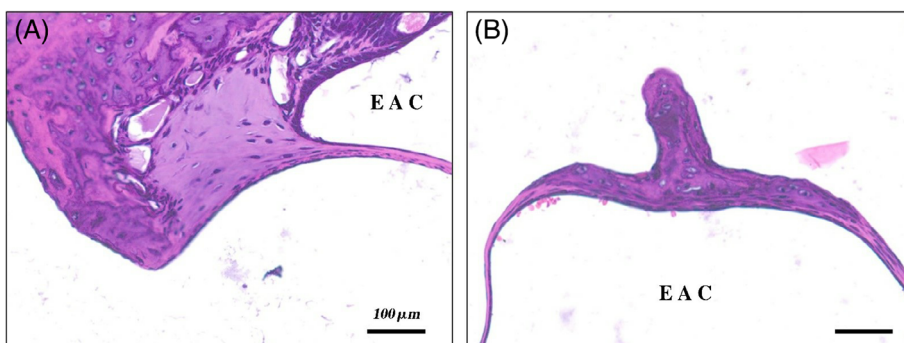


FIGURE 3 High-resolution images of H&E-stained TM sections. The EAC side orientates the images. (A) and (B) show a normal (intact) rat annulus and a malleal handle, respectively. Images were obtained using a panoramic scanner (version 3.0.5; Danjier Electronics Co. Ltd., Jinan, China) at 20 \times magnification. Scale bars: 100 μ m.

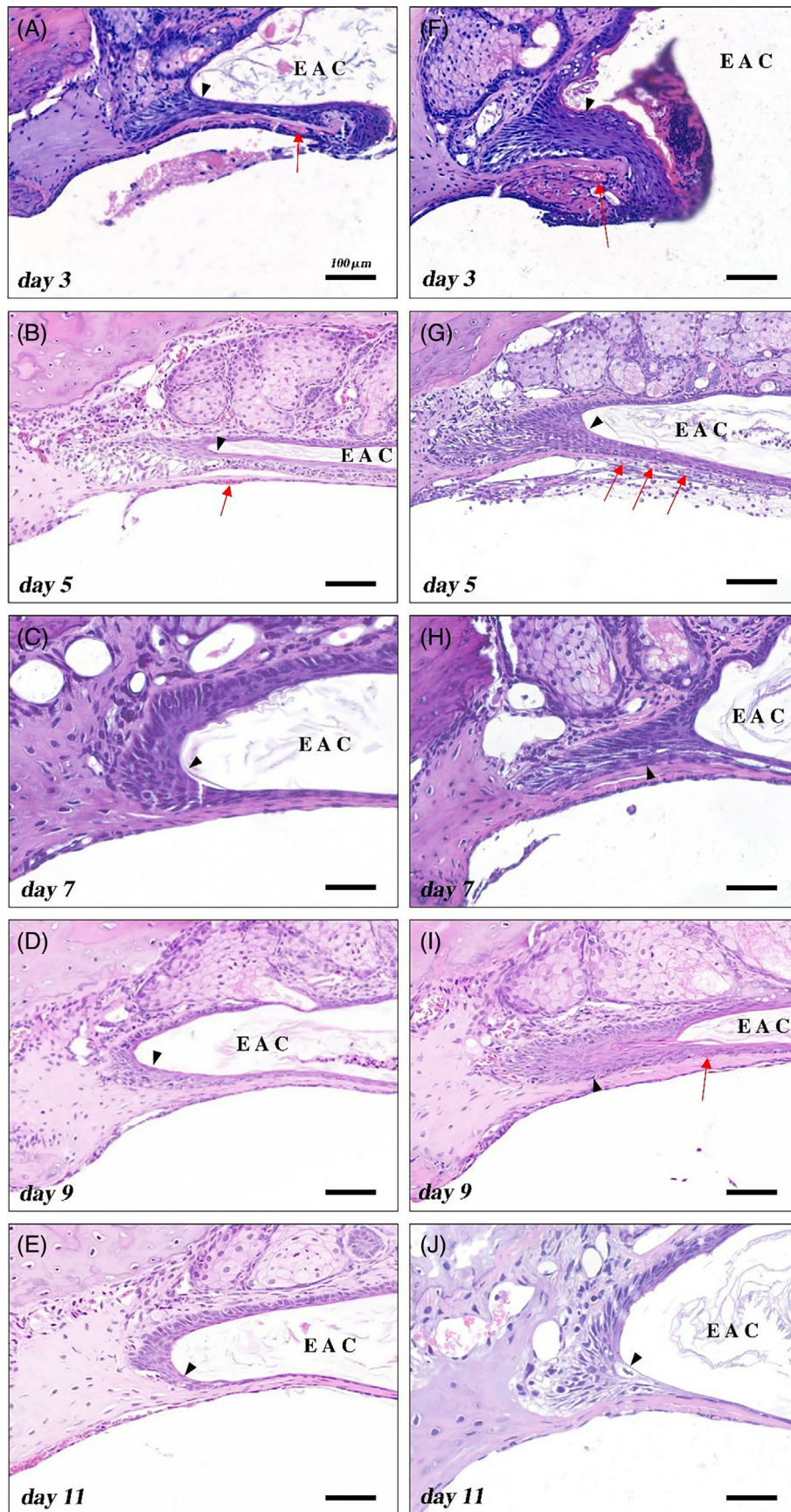


FIGURE 4 High-resolution images of H&E-stained TM sections. The EAC side orientates the images. (A–E) The annulus at various times after perforation in HPEs. (F–J) The annulus at various times after perforation in HEEs. The black triangles indicate the epithelial layers on the side of the annulus. The red arrows indicate blood vessels. Images were obtained using a panoramic scanner (version 3.0.5; Danjier Electronics Co. Ltd.) at 20× magnification. Scale bars: 100 μm.

the annulus. On day 7, a keratinocyte bridge was evident along the line of perforation closure, with a prominent connective tissue layer that contained cells resembling fibroblasts. On day 9, the perforation was macroscopically closed. Keratinocyte proliferation remained active, particularly in the upper half of the annulus, with a thickness of approximately 3–4 cells. Most fibroblasts in the connective tissue layer were disorganized. Collagen fibers remained disorganized on day 11 (Figure 4(F)–(J)).

3.4 | SEM analysis

Three rats each were sacrificed for SEM analysis at 1 month after perforation closure.

Figure 5 presents SEM images of normal and healed TMs with HPE and HEE. Normal TM exhibited a smooth surface and prominent cross arrangement of circular and radial fiber bundles in two directions. However, the healed TM surface showed abundant folds and bumps in bilateral ears. Additionally, the fiber bundles in HPEs were arranged in a direction similar to fiber bundles in the malleus handle; however, they did not exhibit the organized arrangement of normal TMs. The fiber arrangement was completely disorganized in HPEs.

3.5 | ABR testing results

The ABR thresholds of the six rats were determined at the same time points as the morphological analysis. Figure 6(A) shows the ABR

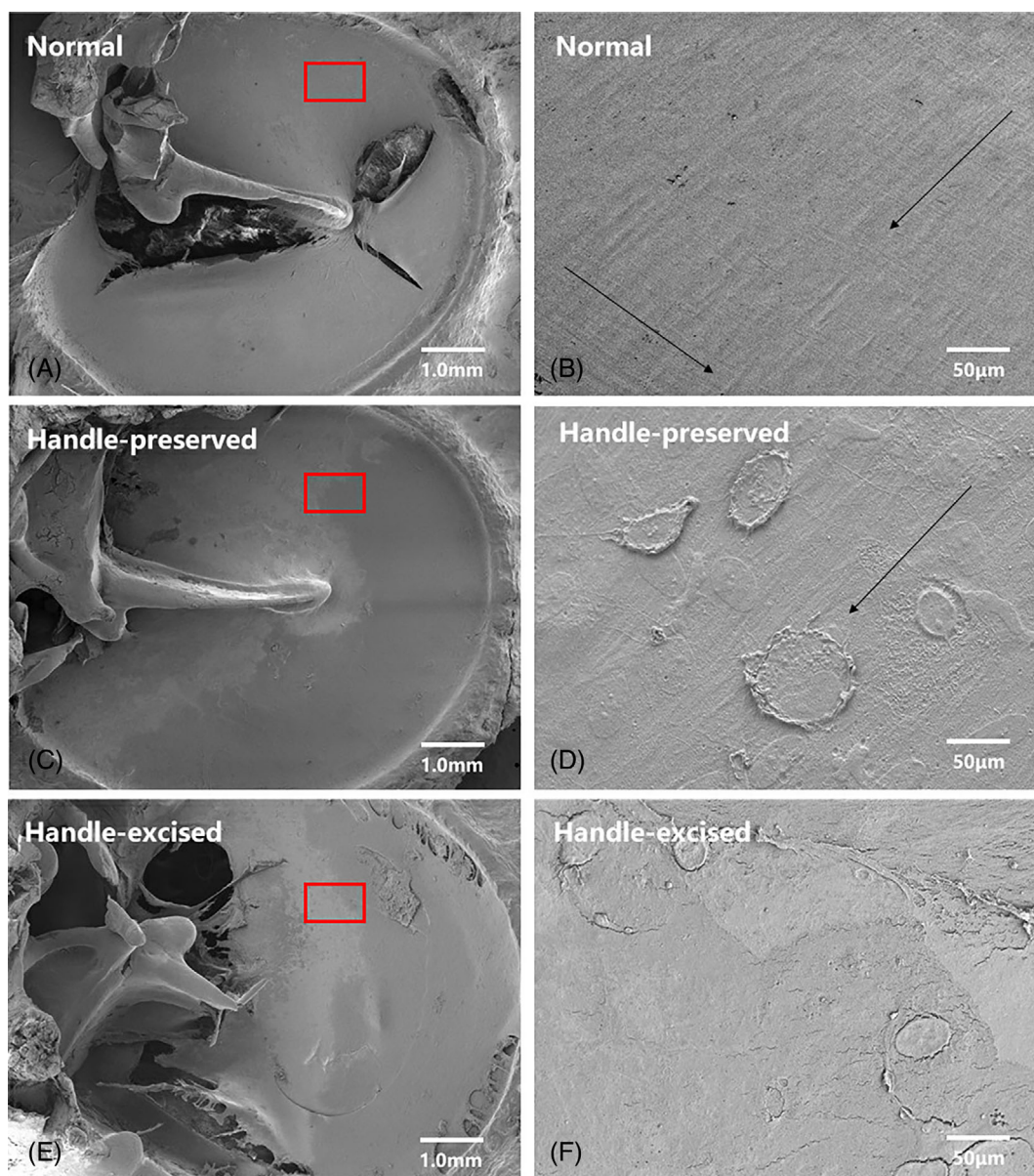


FIGURE 5 SEM images of the TM surface. (A,B) Images of normal TM; (C,D) Images of the HPE; (E,F) Images of the HEE. The black arrow indicates the direction of the collagen fibers; the red box is the designated position the location where the SEM images were acquired.

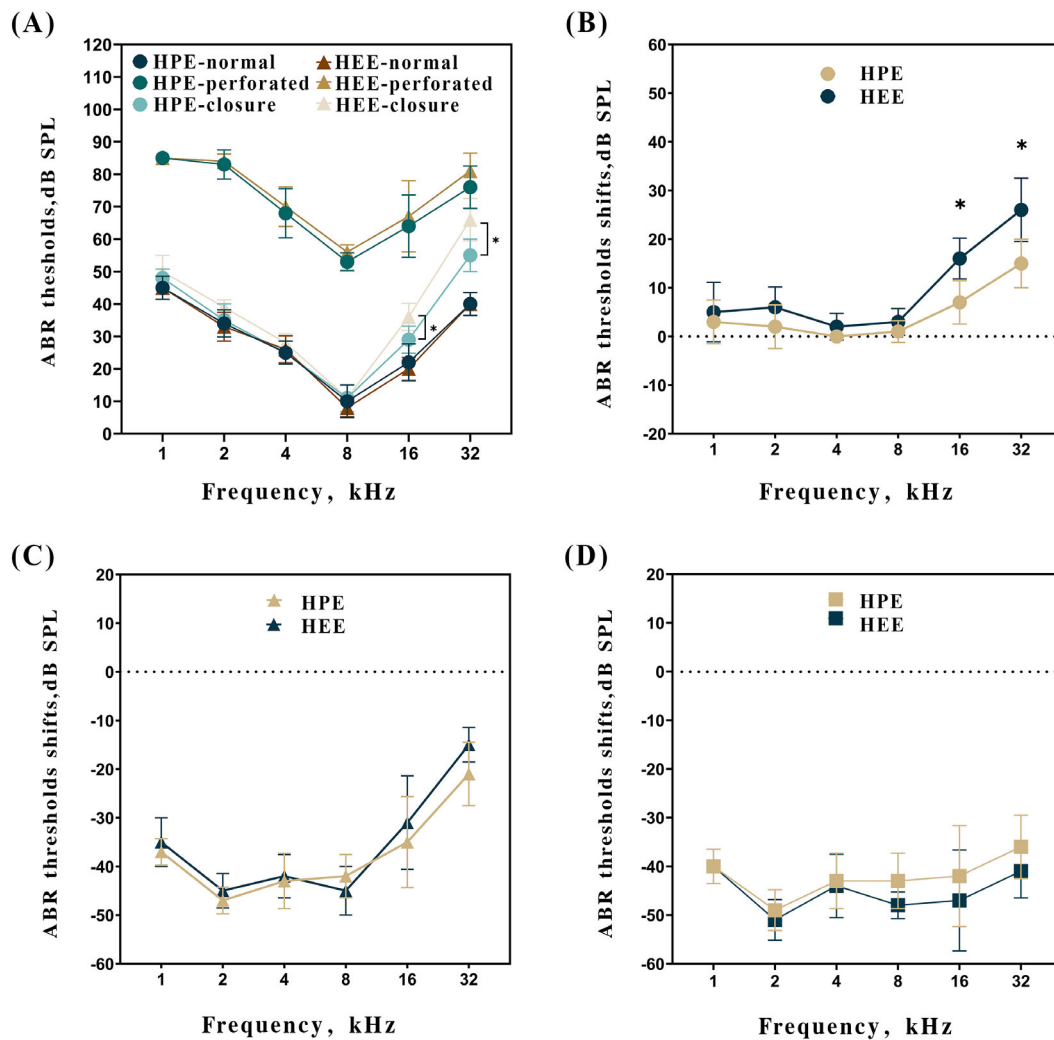


FIGURE 6 ABR thresholds and threshold shifts measured at pre- and post-perforation, and 1 month after perforation among two ears. Number of SD rats: $n = 6$. (A) ABR thresholds of pre- and post-perforation, and 1 month after perforation among two ears ($n = 6$). (B) ABR threshold shifts of pre-perforation and 1 month after perforation among two ears ($n = 6$). (C) ABR threshold shifts of post-perforation and 1 month after perforation among two ears. (D) ABR threshold shifts of pre- and post-perforation ($n = 6$).

thresholds before perforation, after perforation, and 1 month after perforation closure in HEEs and HPEs. At 1 month after perforation closure, the ABR thresholds at 1, 2, 4, and 8 kHz in the HPEs and HEEs were completely recovered to the levels before perforation, whereas the thresholds at 16 and 32 kHz (i.e., high frequencies) were not recovered. Moreover, at 1 month after perforation closure, the ABR thresholds at high frequencies were significantly higher in HEEs than in HPEs (t -test; $p = .029$ at 16 kHz and $p = .017$ at 32 kHz), whereas the thresholds at lower frequencies were similar between HPEs and HEEs. Additionally, there were no significant differences between HPEs and HEEs in terms of the ABR thresholds at any frequency before or after perforation. Figure 6(B) shows the ABR threshold shifts before perforation and 1 month after perforation closure: there were significant differences at high frequencies (t -test; $p = .011$ at 16 kHz and $p = .017$ at 32 kHz) between HPEs and HEEs, but no significant differences were observed at the remaining frequencies. Figure 6(C) shows that no significant differences were

observed in the ABR threshold shift after perforation and 1 month after perforation closure between HPEs and HEEs at any frequency. Figure 6(D) shows there were no significant differences between HPEs and HEEs in the ABR threshold shift at any frequency before or after perforation.

4 | DISCUSSION

In the present study, acute total TM perforations in SD rats closed spontaneously, regardless of excision or preservation of the malleus handle. All perforations closed completely within 6–10 days, and the closure rate did not significantly differ between the ears. However, the presence of the malleus handle showed faster closure, better arrangement of collagen fiber and herein better hearing recovery.

The role of the malleus handle in TM healing is unclear. Some studies have shown that the malleus handle plays an important role in

TM healing,^{2-5,7,8} whereas others have not identified such a role.⁶ In the present study, HPEs had significantly shortened mean closure time, compared with HEEs. Preservation of the malleus handle accelerated the closure of total perforations, presumably because epithelial cell proliferation at the center of the malleus handle aided in the acceleration of perforation closure. Previous studies showed that the epithelial cell proliferation center was located at the malleus handle and the annulus²⁻⁶ or the malleus handle alone.^{7,8} In our study, epithelial layer proliferation began at the annulus on day 3 in both groups. The upper half of the perforation healed more rapidly than the lower half; furthermore, the epithelial layer appeared on the side of the malleus handle by day 5 in HPEs, then formed an epithelial bridge between the umbo and the inferior annulus. These findings suggest that the malleus handle acts as a scaffold for epithelial migration, thereby promoting the migration of epithelial cells along the malleus handle from the upper annulus. Our findings are consistent with the results of a recent study. Frumm et al.¹³ found that the cell progenitors differed between the malleus handle and the annulus. Keratinocyte stem cells were located in a discrete location of the superior TM, whereas the malleus mainly contained migratory committed progenitors. The malleus handle acts as a scaffold to support epithelial migration along the handle. After initial accumulation in the upper half of the annulus, proliferative epithelial cells migrated along the center of the perforation and the handle to both sides of the malleus handle; they subsequently accumulated in the umbo, leading to accelerated perforation closure (Figure 7). The study has the potential to inform the role of the handle of the malleus on mechanisms of epithelial growth on TM perforation and creating effective model of chronic perforation.

Our results suggest that, compared with HEEs, HPEs had expedited and better arrangement of collagen fibers. Collagen fibers became organized and aggregated by day 7 in HPEs, but they remained disorganized on day 11 in HEEs. SEM analysis at 1 month after closure showed that the fiber bundles were radially arranged in the direction of the malleus handle in HPEs, but they were completely disorganized in HEEs. These results showed that the malleus handle promoted the radial arrangement of collagen fiber bundles. Some studies have shown that the network of radial fibers densely converged at the malleus handle and umbo.^{14,15} Additionally, Frumm et al.¹³ found that the long process of the malleus contains committed progenitor clones and platelet-derived growth factor receptor-positive fibroblasts, which promote the migratory and proliferative responses of fibroblasts, as well as extracellular matrix synthesis. These changes promote tissue remodeling, scarring, and fibrosis.^{16,17}

In this study, the malleus handle can be easily removed without impacting the rest of the bone chain. Moreover, no noise producing machine (such as an electrical drill) was used in the whole procedure. Therefore, it is unlikely that the surgery itself produced inner trauma. Based upon the data we could get, however, we cannot rule out the possibility of SNHL due to inner ear damage. This could be verified by testing bone conducted ABR immediately after the surgery. Nevertheless, we did not have facilities to do such a test. Again, we think that such possibility is very small and could be ignored.

There were no significant differences between HPEs and HEEs in the ABR thresholds and the ABR threshold shift at any frequency

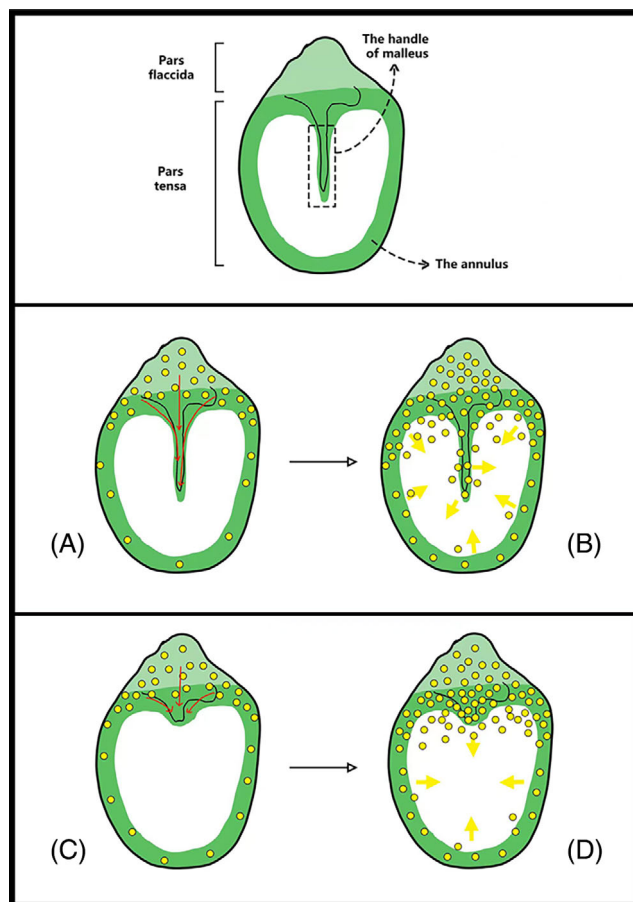


FIGURE 7 Schematic diagram of proliferating epithelial cell migration in the HPE (A and B) and in the HEE (C and D).

before or after perforation in this study. This study showed that high-frequency hearing restoration was better in HPEs than in HEEs. The ABR thresholds recovered to the pre-perforation level in HPEs and HEEs at 1, 2, 4, and 8 kHz at 1 month after perforation closure; however, the high-frequency ABR thresholds (16 and 32 kHz) were not recovered. Nevertheless, preservation of the malleus handle improved the high-frequency hearing, presumably because it allowed the malleus to maintain normal conical shape TM. The conical shape of TM may play a role in high frequency sound conduction. A cone-shaped TM can transfer more force to the ossicles than a flat eardrum, especially at high frequencies. The cone-shaped eardrum allows it to have a larger area for the same canal size, which increases sound transmission to the cochlea.^{18,19} In contrast, absence of the malleus flattened the TM in HEEs, resulting in hearing loss of ≥ 20 dB at high frequencies.¹⁸ It also caused the arrangement of collagen fibers to be better in HPEs than in HEEs, which may contribute to better high-frequency hearing. This notion is supported by previous findings that indicated an integral role for radial collagen fibers in the improvement of high-frequency hearing.^{14,20,21} In addition, for the hearing being lower in the HEEs, this could simply be because of poorer transmission of sound because the mechanical advantage of the ossicular chain has been altered. Therefore, anyway, the malleus handle should be preserved as much as possible in clinic.

The limitation of this study was the absence of the distortion product otoacoustic emission (DPOAE) measurement. Since DPOAE is measured in external ear canal, any conductive hearing loss (such as what is caused by eardrum perforation) could largely attenuate the signal. Therefore, we do not think that DPOAE can provide useful information on the hearing loss and the nature of it. In other words, it would be difficult to interpretate the result of any DPOAE change in this study. Moreover, we did not conduct bone-conducted ABR experiments to determine whether surgery would induce SNHL because of the limitation of the lab setting.

5 | CONCLUSION

Although the malleus handle may not affect the closure of total perforation in SD rats, it contributes to accelerate the perforation closure by possible guide the migration of proliferative epithelial cell on the upper halves of the annulus. Additionally, resection of the malleus handle impairs high frequency hearing recovery following spontaneous closure of the TM.

ORCID

Zihan Lou  <https://orcid.org/0000-0001-8922-6054>

Chunyan Li  <https://orcid.org/0000-0002-8449-9560>

Jingjing Wang  <https://orcid.org/0000-0001-6872-138X>

Zhengkong Chen  <https://orcid.org/0000-0001-7774-441X>

Shankai Yin  <https://orcid.org/0000-0003-3689-8599>

REFERENCES

- Gurov AV, Kryukov AI, Levina JV, Bakhtin AA, Dubovaya TK, Murzakhanova ZV. Hearing dynamics in acute traumatic perforation of the tympanic membrane after application of blood plasma enriched with platelet growth factors. *Vestn Otorinolaringol.* 2021;86(4):23-30.
- Araújo MM, Murashima AA, Alves VM, Jamur MC, Hyppolito MA. Spontaneous healing of the tympanic membrane after traumatic perforation in rats. *Braz J Otorhinolaryngol.* 2014;80(4):330-338.
- Yilmaz MS, Sahin E, Kaymaz R, et al. Histological study of the healing of traumatic tympanic membrane perforation after vivosorb and epifilm application. *Ear Nose Throat J.* 2021;100(2):90-96.
- Schart-Morén N, Mannström P, Rask-Andersen H, von Unge M. Effects of mechanical trauma to the human tympanic membrane: an experimental study using transmission electron microscopy. *Acta Otolaryngol.* 2017;137(9):928-934.
- Goncalves S, Bas E, Goldstein BJ, Angeli S. Effects of cell-based therapy for treating tympanic membrane perforations in mice. *Otolaryngol Head Neck Surg.* 2016;154(6):1106-1114.
- Wang WQ, Wang ZM, Chi FL. Spontaneous healing of various tympanic membrane perforations in the rat. *Acta Otolaryngol.* 2004;124(10):1141-1144.
- Santa Maria PL, Redmond SL, Atlas MD, Ghassemifar R. Histology of the healing tympanic membrane following perforation in rats. *Laryngoscope.* 2010;120(10):2061-2070.
- Kaftan H, Hosemann W, Beule A, Junghans D. An improved animal model for chronic perforation of the tympanic membrane [in German]. *HNO.* 2004;52:714-719.
- Brackmann DE, Sheehy JL, Luxford WM. TORPs and PORPs in tympanoplasty: a review of 1042 operations. *Otolaryngol Head Neck Surg.* 1984;92(1):32-37.
- Shimizu Y, Goode RL. Effect of absence of malleus on ossiculoplasty in human temporal bones. *Otolaryngol Head Neck Surg.* 2008;139(2):301-306.
- Blom EF, Gunning MN, Kleinrensink NJ, et al. Influence of ossicular chain damage on hearing after chronic otitis media and cholesteatoma surgery: a systematic review and meta-analysis. *JAMA Otolaryngol Head Neck Surg.* 2015;141(11):974-982.
- Zhang M, Chen X, Huang Y, Yang Z, Zhang Y, Wu X. The effect of using a PORP to reconstruct the ossicular chain under otoendoscopy with and without a malleus handle. *Acta Otolaryngol.* 2021;141(1):19-22.
- Frumm SM, Yu SK, Chang J, et al. A hierarchy of proliferative and migratory keratinocytes maintains the tympanic membrane. *Cell Stem Cell.* 2021;28(2):315-330.e5.
- O'Connor KN, Tam M, Blevins NH, Puria S. Tympanic membrane collagen fibers: a key to high-frequency sound conduction. *Laryngoscope.* 2008;118(3):483-490.
- Polanik MD, Trakimas DR, Black NL, Cheng JT, Kozin ED, Remenschneider AK. High-frequency conductive hearing following total drum replacement tympanoplasty. *Otolaryngol Head Neck Surg.* 2020;162(6):914-921.
- Sugg KB, Markworth JF, Disser NP, et al. Postnatal tendon growth and remodeling require platelet-derived growth factor receptor signaling. *Am J Physiol Cell Physiol.* 2018;314(4):C389-C403.
- Donovan J, Abraham D, Norman J. Platelet-derived growth factor signaling in mesenchymal cells. *Front Biosci.* 2013;18(1):106-119.
- Fay JP, Puria S, Steele CR. The discordant eardrum. *Proc Natl Acad Sci U S A.* 2006;103(52):19743-19748.
- Razavi P, Tang H, Rosowski JJ, Furlong C, Cheng JT. Combined high-speed holographic shape and full-field displacement measurements of tympanic membrane. *J Biomed Opt.* 2018;24(3):1-12.
- Anand S, Stoppe T, Lucena M, et al. Mimicking the human tympanic membrane: the significance of scaffold geometry. *Adv Healthc Mater.* 2021;10(11):e2002082.
- Li C, Xiong Z, Zhou L, et al. Interfacing perforated eardrums with graphene-based membranes for broadband hearing recovery. *Adv Healthc Mater.* 2022;11(20):e2201471.

How to cite this article: Lou Z, Li C, Yu D, Wang J, Chen Z, Yin S. Comparison of healing of acute total tympanic membrane perforation between rats with and without excision of the malleus handle. *Laryngoscope Investigative Otolaryngology.* 2023;8(6):1648-1656. doi:10.1002/lio2.1175